ELSEVIER

Fuel Processing Technology 77–78 (2002) 453–458

FUEL PROCESSING TECHNOLOGY

www.elsevier.com/locate/fuproc

Kinetics of nitric oxide desorption from carbonaceous surfaces

Alejandro Montoya [a], Fanor Mondragón [a], Thanh N. Truong [b,*]

[a] *Institute of Chemistry, University of Antioquia, Medellín, A.A 1226, Colombia*
[b] *Department of Chemistry, Henry Eyring Center for Theoretical Chemistry, University of Utah, Salt Lake City, UT 84112, USA*

Received 2 February 2002; received in revised form 23 March 2002; accepted 27 March 2002

Abstract

We carried out a molecular modeling study of an important reaction in the combustion of nitrogen-containing chars, the evolution of nitric oxide, (CNO) → NO+(C*). Density functional theory at the B3LYP level was used to provide potential energy surface information and transition state theory was used to provide temperature dependant rate constants. Desorption of NO from nitrogen-containing carbonaceous surfaces is modeled from a pyridine-N-oxide model. The fitted Arrhenius expression for the NO desorption process is $k(T) = 8.84 \times 10^{13} \exp[-42\,132\ \mathrm{K}/T]\ (\mathrm{s}^{-1})$. We found that the rate constants to release CO are slightly larger than rate constants to release NO from the carbonaceous surface. The NO desorption activation energy is 10 kcal/mol lower than that of the CO desorption.

Keywords: Nitric oxide; Carbonaceous surface; Chars

1. Introduction

The heterogeneous mechanism for nitric oxide formation from carbonaceous surfaces can be described as follows:

$$(\mathrm{CN}) + \mathrm{O_2} \rightarrow (\mathrm{CNO}) \rightarrow \mathrm{NO} + (\mathrm{C}^*) \qquad (\mathrm{R.1})$$

Parentheses denote surface-bound species. Basically, a gas-phase oxygen molecule reacts with a surface nitrogen atom of the char to form stable nitrogen–oxygen complexes that

* Corresponding author. Fax: +1-801-581-4353.
E-mail address: truong@mercury.hec.utah.edu (T.N. Truong).

0378-3820/02/$ - see front matter
PII: S0378-3820(02)00080-2

can desorb NO. Thermodynamic and kinetic parameters for the direct NO production channel have been difficult to obtain accurately because some NO can be easily reduced in situ to form N_2 [1]. Therefore, the total NO production is usually approximated from both the direct formation and its reduction on the carbonaceous surface [2,3]. Controlling NO formation from char combustion is a technological issue because it is not mitigated by aerodynamic methods [4]. Then, success in reducing NO evolution depends crucially on the atomic level understanding of the chemical reactions occurring on the nitrogen-containing char surface, hence kinetics and mechanism of the direct NO desorption is very important. The rate of the direct NO production from char-N oxidation is typically assumed to be proportional to the rate of carbon oxidation from char in many single particles models [3]. However, a time-resolve study in a transient state shows that the activation energy for the direct NO desorption is in the range of 3–5 kcal/mol [5], while activation energy for CO desorption obtained from temperature programmed desorption is in the range of 80–85 kcal/mol at high temperatures [6]. Although different experimental procedures were used in both cases, different hypotheses for the large difference in activation energy may be considered, i.e., because an incomplete desorption channel from nitrogen–oxygen complexes was used or simply because the desorption mechanisms are different.

In previous studies, we began an investigation on the mechanism and kinetics of CO desorption from carbonyl and semiquinone carbon–oxygen complexes [7,8]. Our predicted rate constants are within the uncertainty of available experimental data indicating that the direct ab initio dynamics approach can be used to provide necessary thermodynamic and kinetic properties of important reactions in char oxidation processes. Therefore, in the present paper, we employed the direct ab initio dynamics method to study the mechanism and kinetics of desorption of nitric oxide from nitrogen-containing chars. A direct comparison of the mechanism of NO desorption with existent data for CO desorption processes will increase our understanding on the char-N chemistry that could help us to design better processes to mitigate its adverse effects in global warming and in stratospheric ozone depletion.

2. Results and discussion

Several nitrogen functionalities present on oxidized char surfaces have been established, namely pyrrole, pyridine, quaternary nitrogen and N-oxide functionalities such as pyridone and pyridine-N-oxide [9]. As a case study, NO desorption reaction was modeled using a pyridine-N-oxide on a five six-member ring carbon model in zigzag shape as shown in Fig. 1. Unsaturated carbon atoms at the edge of the carbon model were used to represent the active sites of the char. The pyridine-N-oxide complex was optimized in C_{2v} symmetry at the B3LYP DFT level of theory [10] using the 6–31G(d) basis set. We have performed several optimizations for different electronic states to determine the ground state. Electronic calculations were done using the Gaussian 98 program [11].

Selected optimized geometrical parameters and the Wiberg bond order index [12], which is related to the strength of the bond, are shown in Fig. 1. As can be seen, the N–O bond order index is the highest in the N-oxide model, then it is expected that a NO

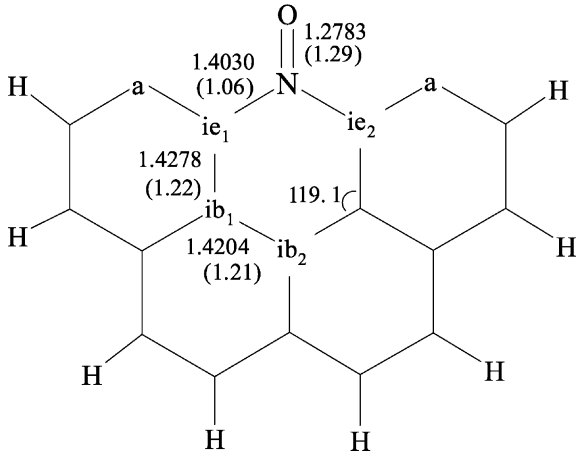

Fig. 1. Pyridine-N-oxide model in zigzag shape. Some carbon atoms are named to facilitate the discussion. (a) Active carbon atom, (ie) inactive exposed carbon atom, (ib) inactive buried carbon atom. Selected optimized bond length in angstroms (Å). Numbers in parenthesis are Wiberg bond order indexes.

molecule might be released by breaking the two $N-C_{ie1(ie2)}$ bonds. The equilibrium pyridine-N-oxide complex was found to have two low-lying electronic states; the doublet excited state is 3.9 kcal/mol higher than the quartet ground state. At combustion temperatures, one can expect that both electronic states are populated. It was found that the NO desorption energy barrier on the quartet electronic state is 146.7 kcal/mol, while the energy barrier on the doublet electronic state is 86.8 kcal/mol. Thus, it is reasonable to assume that the desorption process would occur mostly on the doublet surface. Desorption of nitric oxide is modeled by pulling the NO group away from the carbon model while maintaining the doublet electronic state. To estimate the energy profile for this process, we calculated the NO desorption potential energy curve as function of the reaction coordinate, namely the $C_{ib2}-N$ distance, starting from its equilibrium value to 7 Å at the interval of 0.2 Å, while relaxing other degrees of freedom. The zero point corrected NO desorption potential energy curve on the doublet electronic state is shown in Fig. 2, as well as the $C_{ie1}-C_{ie2}$ distance. The NO desorption route proceeds with an energy barrier of 78.2 kcal/mol and the backward reaction barrier is 39.4 kcal/mol. Notice that in the initial stage of the desorption, the ring opens slightly to let NO break away; and then closes up to form a five-member ring. The geometry of the activated nitrogen–oxygen complex that corresponds to the highest point in the energy curve is shown in Fig. 3. The model was fully optimized and selected optimized geometrical parameters and the Wiber bond order indexes are depicted in the same figure. It is seen that while the NO bond is 64% stronger than the corresponding bond in the pyridine-N-oxide complex, the $N-C_{ie1}$ bond is 90% weaker due to the desorption process. The activated complex involves a planar six-member ring with partial bonding between the carbon–nitrogen–carbon.

Thermal rate constant for the direct NO production was calculated at the Transition State Theory (TST) using the Virtual Kinetic Laboratory [13]. A normal mode analysis on the activated complex shows that the transition state structure for the NO desorption

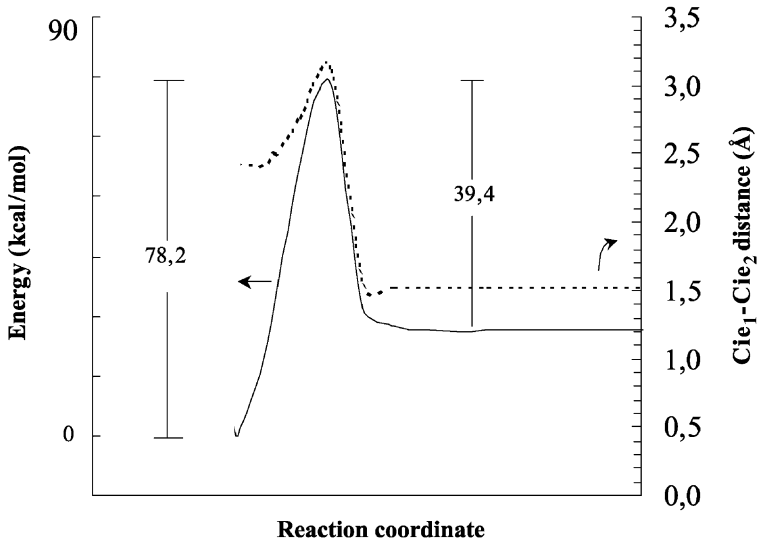

Fig. 2. Doublet-state potential energy curve and the $C_{ie1}-C_{ie2}$ distance for the NO desorption channel of reaction.

channel is non-planar. Vibrational partitional functions were calculated quantum-mechanically within the harmonic approximation while translational and rotational partition functions were computed classically. Both the doublet and quartet states were included in calculations of the reactant electronic partition function. The calculated forward rate

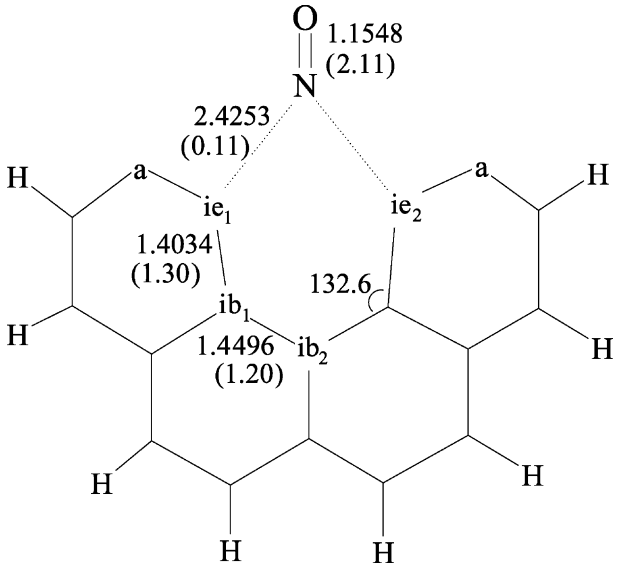

Fig. 3. Activated nitrogen–oxygen complex that leads to the NO desorption molecule. Bond lengths in angstroms (Å) and angles in degrees. Numbers in parenthesis are Wiberg bond order indexes.

Table 1
Transition state rate constant (s^{-1}) for NO and CO desorption from a carbonaceous model at different temperatures (K)*

Temperature	NO desorption	CO desorption	NO/CO ratio
800	1.20×10^{-9}	1.73×10^{-9}	6.94×10^{-1}
900	4.40×10^{-7}	1.14×10^{-6}	3.86×10^{-1}
1000	4.88×10^{-5}	2.14×10^{-4}	2.28×10^{-1}
1100	2.29×10^{-3}	1.59×10^{-2}	1.44×10^{-1}
1200	5.59×10^{-2}	5.90×10^{-1}	9.47×10^{-2}

* CO desorption rate constant obtained from the scientific literature [8].

constants were obtained on the doublet electronic state. The fitted Arrhenius expression for the present NO calculated rate constants is $k(T) = 8.84 \times 10^{13} \exp[-42\,132\ \mathrm{K}/T]$ (s^{-1}). Table 1 shows the transition state rate constant for the NO and CO desorption at different temperatures. The theoretical CO desorption rate constant was obtained from our previous study [8] and it is included here just for comparison purposes. A direct comparison of the NO and CO desorption rate constant can be done because they are obtained at the same level of theory and using the same carbonaceous model. It can be seen that desorption rate constant for CO is slightly larger than the NO desorption rate constant. The difference in the rate constant becomes bigger as the temperature increases. Notice that the activation energy obtained from the Arrhenius expression is 83.8 and 94.3 kcal/mol with smaller frequency factors for NO desorption. Then, increasing the temperature, the rate constant ratio (NO/CO) shown in Table 1 decreases. At higher temperatures, there is a small selectivity to release carbon atoms first while the selectivity decrease at lower temperatures.

3. Conclusions

Major discrepancies between theoretical and experimental activation energies for the NO desorption have been found in this study. However, the desorption rate constants of NO and CO are not considerably different as it has been assumed in single particle models [3]. The hypothesis that NO can be released by a different mechanism from that of CO is not supported from this study. Then, it is necessary to consider other types of NO precursors to have a complete insight into the overall NO desorption process. Nevertheless, considering that the pyridine-N-oxide model is a plausible NO precursor with a high NO desorption activation energy shows that it has an important effect on the rate-limiting step on the mechanism of the direct uncatalyzed NO production. Clearly, additional work is needed on the NO formation from the (CNO) surface complexes.

Acknowledgements

T.N. Truong acknowledges financial support from NSF and University of Utah. F. Mondragón and A. Montoya want to thank the University of Antioquia for financial

support of the project IN408CE. We also thank the Utah Center for High Performance computing for computer time support.

References

[1] K.M. Thomas, Fuel 76 (6) (1997) 457–473.
[2] J.O.L. Wendt, O.E. Schulze, AIChE J. 22 (1) (1976) 102–110.
[3] S.P. Visona, B.R. Stanmore, Combust. Flame 106 (3) (1996) 207–218.
[4] E.G. Eddings, P.J. Smith, M.P. Heap, D.W. Pershing, A.F. Sarofim, Coal-blending and switching of low-sulfur western coals, ASME (1994) 169–184.
[5] G.G. De Soete, E. Croiset, J.R. Richard, Combust. Flame 117 (1/2) (1999) 140–154.
[6] K.J. Huettinger, J.S. Nill, Carbon 28 (4) (1990) 457–465.
[7] A. Montoya, T.-T.T. Truong, F. Mondragon, T.N. Truong, J. Phys. Chem., A 105 (27) (2001) 6757–6764.
[8] A. Montoya, F. Mondragón, T.N. Truong, J. Phys. Chem., A 106 (16) (2002) 4236–4239.
[9] J.R. Pels, F. Kapteijn, J.A. Moulijin, Q. Zhu, K.M. Thomas, Carbon 33 (11) (1995) 1641–1653.
[10] A.D.J. Becke, Chem. Phys. 98 (7) (1993) 5648–5652.
[11] M.J. Frisch, G.W. Trucks, H.B. Schlegel, G.E. Scuseria, M.A. Robb, J.R. Cheeseman, et al., Gaussian 98, Rev. A.9, Pittsburgh, PA, 1998.
[12] K.B. Wiberg, Tetrahedron 24 (3) (1968) 1083–1096.
[13] S. Zhang, T.N. Truong, http://vklab.Hec.Utah.Edu. Vklab, version 1.0, 2001.